NIH Public Access
Author Manuscript
Pharm Res. Author manuscript; available in PMC 2014 March 25.

Published in final edited form as:
Pharm Res. 2014 February ; 31(2): 466–474. doi:10.1007/s11095-013-1175-4.

Zanamivir conjugated to poly-*L*-glutamine is much more active against influenza viruses in mice and ferrets than the drug itself

Alisha K. Weight[a], **Jessica A. Belser**[b], **Terrence M. Tumpey**[b], **Jianzhu Chen**[c], and **Alexander M. Klibanov**[a,d]

Jianzhu Chen: jchen@mit.edu; Alexander M. Klibanov: klibanov@mit.edu

[a]Department of Chemistry, Massachusetts Institute of Technology, Cambridge, MA 02139

[b]Influenza Division, National Center for Immunization and Respiratory Disease, Centers for Disease Control and Prevention, Atlanta, GA 30333

[c]Department of Biology and David H. Koch Institute for Integrative Cancer Research, Massachusetts Institute of Technology, Cambridge, MA 02139

[d]Department of Biological Engineering, Massachusetts Institute of Technology, Cambridge, MA 02139

Abstract

Purpose—Previously, polymer-attached zanamivir had been found to inhibit influenza A viruses *in vitro* far better than small-molecule zanamivir itself. The aim of this study was to identify *in vitro* – using the plaque reduction assay - a highly potent zanamivir-polymer conjugate, and subsequently test its antiviral efficacy *in vivo*.

Methods—By examining the structure-activity relationship of zanamivir-polymer conjugates in the plaque assay, we have determined that the most potent inhibitor against several representative influenza virus strains has a neutral high-molecular-weight backbone and a short alkyl linker. We have examined this optimal polymeric inhibitor for efficacy and immunogenicity in the mouse and ferret models of infection.

Results—Zanamivir attached to poly-*L*-glutamine is an effective therapeutic for established influenza infection in ferrets, reducing viral titers up to 30-fold for 6 days. There is also up to a 190-fold reduction in viral load when the drug is used as a combined prophylactic/therapeutic in mice. Additionally, we see no evidence that the drug conjugate stimulates an immune response in mice upon repeat administration.

Conclusions—Zanamivir attached to a neutral high-molecular-weight backbone through a short alkyl linker drastically reduced both *in vitro* and *in vivo* titers compared to those observed with zanamivir itself. Thus further development of this polymeric zanamivir for the mitigation of influenza infection seems warranted.

Keywords

influenza virus; mouse model of infection; ferret model of infection; polymeric antiviral agents; zanamivir

INTRODUCTION

Influenza is a persistent and constantly evolving threat to global human health. Despite annual vaccinations, hundreds of millions of people are infected and hundreds of thousands die from the infection each year (1,2). Prophylactic seasonal immunization against viral hemagglutinin antigens relies on accurate prediction of future circulating strains. Broader-

NIH-PA Author Manuscript
NIH-PA Author Manuscript
NIH-PA Author Manuscript

NIH-PA Author Manuscript

NIH-PA Author Manuscript

NIH-PA Author Manuscript

spectrum small molecule inhibitors targeting minor surface antigens are currently approved for prophylactic and/or therapeutic administration. The utility of these two M2 ion-channel inhibitors and two neuraminidase inhibitors - Tamiflu (oseltamivir) and Relenza (zanamivir) - continues to diminish due to viral mutations (3,4). In fact, since 2006 the U.S. Food and Drug Administration (FDA) has advised physicians not to prescribe the M2 ion-channel inhibitors because most circulating influenza viruses have acquired resistance to them (5). Although the search for new small-molecule inhibitors is ongoing (5–8), identifying compounds with high potency (ideally low-nM inhibitory concentrations) has been only moderately successful.

One promising avenue has been the chemical modification of zanamivir (**1**) itself. Specifically, its 7-*O*-alkyl-ether derivatives were tested in cell-based assays for inhibition of influenza virus infection (9–11). The most efficacious of these analogues were conjugated to a polymeric scaffold and exhibited enhanced antiviral action compared to small-molecule **1**-based parent compounds (9,10). However, few studies have examined the structure-activity relationship (SAR) for **1**-derivatized polymeric inhibitors in *in vitro* antiviral assays or, more importantly, their antiviral activity *in vivo*.

Previously, we have identified conjugate **5a** – poly-*L*-glutamine containing 10 mol-percent of a **1**'s 7-*O*-alkyl-carbamate analog **2** (Figure 1) – as a drug candidate that fills two unmet needs: it (i) is a potent inhibitor of drug-resistant strains of influenza viruses (12) and (ii) has two modes of action inhibiting both neuraminidase activity and fusion of endosomes with the virus (13). In the present work, we have pursued *in vitro* SAR studies of polymer conjugates of **1** to identify the most efficacious candidate; the latter has been subsequently examined *in vivo* in the mouse and ferret models of influenza infection.

MATERIALS AND METHODS

Reagents

Poly-*L*-glutamic acid Na salt (MW 50–100 kDa) and all other chemicals, biochemicals, and solvents were purchased from Sigma-Aldrich Chemical Co. (St. Louis, MO) unless otherwise noted and used without further purification.

Synthesis and characterization

Drug **1** was obtained from BioDuro (Beijing, China). Small molecule **2**, poly-*L*-glutamine (**5**), and **5**-attached **1** (**5a and 5d**) were synthesized by us as described previously (12,14,15).

3-Acetamido-2-(1-(((2-(2-aminoethoxy)ethyl)carbamoyl)oxy)-2,3-dihydroxypropyl)-4-guanidino-3,4-dihydro-2H-pyran-6-carboxylic acid (3) was synthesized using a modified literature procedure (14,15) with *tert*-butyl-(2-(2-aminoethoxy)ethyl)carbamate (ChemPep, Wellington, FL) to introduce the linking group. Subsequent reduction/deprotection with triphenyl phospine/triethylamine/H_2O and guanidinylation with *N,N'*-bis-*tert*-butoxycarbonyl-1H-pyrazole-1-carboxamidine of intermediates were performed as previously described (14,15) with modification to the purification schemes. For both intermediates, purification was done using a reverse-phase silica plug (Sep Pak C18 cartridge vac 6cc, Waters, Milford, MA). Crude intermediates were loaded in water and 1:4 (v/v) water:methanol, respectively. Product was eluted with 12 mL of water followed by either 15% acetonitrile or 40% methanol, respectively. BOC-deprotection was performed as previously described (14,15) to give compound **3**. ^{1}H NMR (D_2O) δ (500 MHz) – 1.85 (3H, s, CH_3CONH), 3.05–3.25 (4H, m, -NHCH$_2$*CH$_2$*O*CH$_2$*CH$_2$NH$_2$), 3.40 (1H, dd, H-9$_a$), 3.50 (2H, m, -NH*CH$_2$*CH$_2$OCH$_2$CH$_2$NH$_2$), 3.60 (1H, d, H-9$_b$), 3.65 (2H, m, -

NIH-PA Author Manuscript

NIH-PA Author Manuscript

NIH-PA Author Manuscript

$NHCH_2CH_2OCH_2CH_2NH_2$), 3.95 (1H, m, H-8), 4.05 (1H, t, H-5), 4.35 (1H, d, H-4), 4.45 (1H, d, H-6), 4.90 (1H, d, H-7), 5.95 (1H, d, H-3).

3-Acetamido-2-(1-(((4-(aminomethyl)phenyl)carbamoyl)oxy)-2,3-dihydroxypropyl)-4-guanidino-3,4-dihydro-2H-pyran-6-carboxylic acid (4) was synthesized analogously to **3** above using *tert*-butyl-4-aminobenzylcarbamate to introduce the linker group. ^{1}H NMR (D_2O) δ (500 MHz) – 1.85 (3H, s, CH_3CONH), 3.45 (1H, q, H-9_a), 3.60 (1H, d, H-9_b), 4.10–4.20 (2H, m, H-5 and H-8), 4.35–4.45 (3H, m, PhCH_2NH_2 and H-4), 4.50 (1H, d, H-6), 5.0 (1H, d, H-7), 5.85 (1H, d, H-3), 7.25–7.35 (4H, m, aromatic).

Polymer conjugates 5b and 5c were synthesized analogously to **5a** (9), with subsitution of **3** or **4**, respectively, for small molecule **2**. Briefly, 12 mole percent of **3** or **4** were added to hydroxybenzotriazole-activated poly-*L*-glutamic acid. After addition of catalytic pyridine, the reaction was stirred at room temperature for 24 h and quenched with aqueous NH_4OH for an additional 24 h. The reactions were then diluted with distilled water and buffer exchanged into the same at least four times before lyophilization. ^{1}H NMR (D_2O) δ (500 MHz) – For **5b**: 1.8–2.1 (5H, m, 2H polymer and CH_3CONH), 2.1–2.4 (2H, d, 2H polymer), 3.0–3.2 (4H, m, $NHCH_2CH_2OCH_2CH_2NH_2$), 3.35–3.45 (2H, m, $NHCH_2CH_2OCH_2CH_2NH_2$), 3.45 (1H, dd, H-9_b), 3.55 (1H, d, H-9_a), 3.6 (2H, m, $NHCH_2CH_2OCH_2CH_2NH_2$), 3.95 (1H, m, H-8), 4.05–4.25 (2H, s, 1H polymer and H-5), 4.45 (1H, d, H-4), 4.55 (1H, d, H-6), 5.7 (1H, s, H-3). For **5c**: 1.9–2.1 (5H, m, 2H polymer and CH_3CONH), 2.2–2.4 (2H, d, 2H polymer), 3.5 (1H, q, H-9_a), 3.6 (1H, dd, H-9_b), 4.1–4.35 (9H, m, 4H polymer, H-4, H-5, H-8, PhCH_2NH_2), 4.5 (1H, d, H-6), 5.7 (1H, d, H-3), 7.3 (4H, m, 4H aromatic)

Conjugate 6a and scaffold 6. Conjugate **6a** was synthesized analogously to **5a** (9,12) using 3 mL of 0.1 M NaOH to quench the polymer conjugation reaction for 48 h at RT. Underivatized **6** was synthesized by quenching benzotriazole-activated poly-*L*-glutamate with an excess of 0.1 M NaOH. After quenching, both reactions were diluted with distilled water and buffer-exchanged into the same at least four times using an Amicon Ultra Centrifugal Filter with an Ultracel regenerated cellulose membrane (15 mL, 15 kDa MW cutoff) at 4,000 × *g* before lyophilization. ^{1}H NMR (D_2O) δ (500 MHz) – For **6a**: 1.1–1.4 (8H, m, -$NHCH_2(CH_2)_4CH_2NH_2$), 1.7–2.4 (7H, m, 4H polymer and CH_3CONH), 2.8–3.05 (4H, m, -$NHCH_2(CH_2)_4CH_2NH_2$), 3.5 (1H, dd, H-9_b), 3.6 (1H, d, H-9_a), 3.8 (2H, m, H-5, H-8), 4.1–4.25 (1H, s, 1H polymer), 4.45 (1H, d, ZA), 4.55 (1H, d, H-6), 5.0 (1H, d, H-7), 5.75 (1H, s, H-3). For **6**: 1.7–2.3 (4H, m, 4H polymer), 4.2 (1H, s, 1H polymer).

Conjugate 7a and scaffold 7. Attachment of **2** to the activated polymer scaffold was performed analogously to **5a** (9,12). After 4 h, the reaction was cooled on an ice bath. Solid *N*-ethyl-*N*'-(3-dimethylaminopropyl)carbodiimide hydrochloride (2.72 mg, 0.0142 mmol, 1.2 eq) was added to the reaction mixture, which was subsequently purged with argon gas. A solution of 4-dimethylaminopyridine (0.072 mg, 0.00059 mmol, 0.05 eq) in DMF (15 μL) was then added, and the mixture was stirred for 5 min. A pre-cooled solution of choline chloride (6.59 mg, 0.0472 mmol, 4 eq) in formamide (240 μL to give its final concentration in the reaction mixture of 30% (v/v)) was then added dropwise. The reaction mixture was stirred on ice for 16 h and allowed to warm to RT overnight. Bare **7** was synthesized by directly quenching benzotriazole-activated poly-*L*-glutamate with choline chloride in formamide as described above. After quenching, both reaction mixtures were diluted with distilled water and buffer-exchanged into the same at least four times using an Amicon Ultra Centrifugal Filter with a regenerated cellulose membrane (15 mL, 15 kDa MW cutoff) at 4,000 × *g* before lyophilization. ^{1}H NMR (D_2O) δ (500 MHz) – For **7a**: 1.2–1.5 (8H, m, -$NHCH_2(CH_2)_4CH_2NH_2$), 2.0–2.8 (7H, m, 4H polymer and CH_3CONH), 2.9–3.05 (4H, m, -$NHCH_2(CH_2)_4CH_2NH_2$), 3.2 (9H, s, -$N(CH_3)_3$), 3.5 (1H, dd, H-9_a), 3.55 (1H, d, H-9_b), 3.7

NIH-PA Author Manuscript

NIH-PA Author Manuscript

NIH-PA Author Manuscript

(2H, s, -CH_2N-) 4.05 (2H, m, H-8 and H-5), 4.1–4.3 (2H, 1H polymer and H-4), 4.5 (1H, d, H-6), 4.55 (2H, s, -CH_2O-), 5.65 (1H, s, H-3). For **7**: 2.0–2.8 (4H, m, 4H polymer), 3.25 (9H, s, -N(CH_3)$_3$), 3.8 (2H, s, -CH_2N-), 4.15–4.4 (1H, s, 1H polymer), 4.65 (2H, s, CH_2O-).

Plaque reduction assay

The plaque reduction assay to determine inhibitory constants of small-molecule and polymeric inhibitors was performed as previously described (12). Briefly, virus dilutions in PBS were incubated with an equal volume of inhibitor dilutions in PBS (serially 10-fold diluted) for 1 h at room temperature. Confluent MDCK cell monolayers were incubated at room temperature for 1 h. The inoculum was removed by aspiration and the cells overlaid with agar medium. Plaques were counted after 3 and 4 days of incubation at 37°C.

Influenza viruses

Plaque-purified influenza A/WSN/33 (WSN; H1N1) was cultured in E4HG medium from MDCK cells (ATCC; Manassas, VA), clarified, and filtered through a 0.2-μm filter to remove aggregates. Influenza virus strains A/Wuhan/359/95 (Wuhan; H3N2), A/turkey/MN/833/80 (TKY; H4N2), and A/turkey/MN/833/80/E119D drug-resistant mutant (TKY E119D) were obtained from the Centers for Disease Control and Prevention (CDC) (Atlanta, GA) and propagated as previously described (14). Sucrose-gradient purified influenza A/PR/8/34 (PR8; H1N1) was obtained from Charles River Laboratories in HEPES-saline buffer (Wilmington, MA) and diluted with PBS (pH 7.2) before use. Titers were determined by serial titration in the plaque assay (12). Stocks of influenza A/Nanchang/933/95 (Nanchang) H3N2 virus were grown in the allantoic cavities of 10-day-old embryonated hens' eggs at 34°C for 48–72 h. Pooled allantoic fluid was clarified by centrifugation and stored at −70°C. Fifty percent egg infectious dose (EID_{50}) titers were determined by serial titration of virus in eggs and calculated by the method of Reed and Muench (16).

Ethics statement

All mice were housed at the Animal Facility of the Massachusetts Institute of Technology (MIT), and all studies with them were performed in accordance with the institutional guidelines. All mouse procedures were approved by the MIT Committee on Animal Care under protocol #0310-027-13. The ferret study was carried out in strict accordance with recommendations in the Guide for the Care and Use of Laboratory Animals of the National Institutes of Health. All ferret procedures were approved by the CDC Institutional Animal Care and Use Committee (IACUC) and in a facility accredited by the Association for Assessment and Accreditation of Laboratory Animal Care International. Animal studies were performed in accordance with the IACUC guidelines under protocol #2195TUMFERC-A3: "Studies on the Pathogenesis and Transmission of Recombinant Influenza Viruses in Ferrets".

Mouse experiments

Male Balb/C mice at 8 weeks (Jackson Laboratories, Bar Harbor, ME) were used in this study. They were anesthetized with intraperitoneal avertin injection and dosed intranasally in one nostril with a 25-μL solution of PBS (vehicle control), **1**, high-molecular-weight **5**, or high-molecular-weight **5a**. Within 10 min, mice were then infected with 25 μL of a virus solution in PBS (1,000 pfu/mouse) delivered in the same nostril. At 6, 24, and 48 h post-infection (p.i.), mice were again given PBS, **1, 5**, or **5a**.

Inhibitor doses were 0.028 μmol/kg for **1**, an equimolar dose of **5a** (0.028 μmol/kg on a **1** basis; 0.24 μmol/kg on a monomer basis), and 11 μmol/kg **5** (40-fold molar equivalency on a monomer basis). Group sizes were: PBS – 6 mice, **5** – 3 mice, **5a** – 4 mice, and mock

NIH-PA Author Manuscript

NIH-PA Author Manuscript

NIH-PA Author Manuscript

infection – 3 mice. For WSN-infection, 5 mice were given **1**. For PR8-infection, 6 mice were given **1**. Animals were euthanized with CO_2 at 72 h p.i. Whole mouse lung was harvested, rinsed in ice-cold homogenization buffer (50 mL of PBS plus 150 μL of 35% BSA and 500 μL of a solution of 10,000 IU/mL penicillin G and 10,000 mg/mL streptomycin (JR Scientific, Woodland, CA)), flash-frozen on dry ice in 1 mL of ice-cold homogenization buffer, and stored at −80°C until processing.

For PR8-infected mice, lungs were homogenized using a Branson Sonifier 250 with a ⅛" tapered tip probe (Branson Ultrasonics, Danbury, CT). Total RNA was extracted from 170 μL of clarified lung homogenate using the PureLink Viral RNA/DNA Kit (Invitrogen, Carlsbad, CA) according to manufacturer's instructions. Viral RNA was eluted in Tris-EDTA buffer (pH 8.0) and stored at −80°C. Quantification of viral RNA was performed using the RNA Ultrasense One-step qRT-PCR System (Invitrogen) according to manufacturer's instructions after treatment with RNase-free DNase (Ambion, Austin, TX). Primer and probe to detect the encoding region for the M1 matrix protein were used at concentrations of 1,900 nM and 754 nM, respectively, in a total reaction volume of 40 μL. Sequences of influenza-specific primers and probe (IDT, Coralville, IA) were previously established (17). A Roche LightCycler® instrument was used for real-time reverse-transcriptase PCR using the following program: 45°C for 30 min, 95°C for 2 min, and 50 cycles of 95°C for 5 sec, 55°C for 10 sec, and 72°C for 10 sec. All samples and a standard curve of serially diluted un-passaged virus were run on the same reaction plate. Levels of viral RNA in lung homogenates (18) are expressed as threshold cycle (C_T), determined using LightCycler® 480 System software v. 1.5. To verify that any residual polymer in homogenates did not interfere with RNA extraction, a sample of stock virus and a sample of homogenate from an untreated mouse were spiked with **5** before extraction and PCR. A standard curve of the spiked virus and C_T value of the spiked homogenate were in agreement with that of the un-passaged virus. Thus, the observed C_T values reflect robust purification.

For WSN-infected mice, their lungs were homogenized using a Dounce homogenizer on ice. Viral titers of WSN in clarified murine lung homogenates were determined by 12-well format plaque assay and expressed in pfu/mL (12,14,19). To exclude the possibility that the reduced titers measured in treated groups were a result of residual **1** or **5a** in lung homogenates, one uninfected mouse was dosed with each inhibitor. Lung homogenates from these mice were mixed in equal volume with that of infected but untreated (PBS control) mice. No significant difference in virus titer was observed; the reduction in titer seen with treated mice does indeed reflect *in vivo* inhibition.

Immune response studies were performed with 8-week old male Balb/C mice. Mice were divided into two groups of four, anesthetized with intraperitoneal avertin, and challenged with 40 μL of PBS or 40 μL of 1 mg/mL high-molecular-weight **5a** at 0, 6, 24, and 48 h. After 4 weeks, mice were re-challenged with three administrations of 40 μL of PBS or 40 μL of 1 mg/mL **5a**. Serum samples were collected "pre-challenge" from a tail-vein 3 weeks before initial challenge. "Primary challenge" and "secondary challenge" samples were collected 10 days after initial challenge and secondary challenge. Serum samples were separated using BD Microtainer serum separator tubes (Becton Dickinson, Franklin Lakes, NJ) and stored at −80°C.

ELISA

ELISA experiments to determine total and specific immunoglobulin levels in mouse serum were performed according to a modified literature procedure using Costar Universal Bind plates (Corning, Tewksbury, MA) (13). Antibody pairs and standards (mouse IgG, IgM, and IgA) and TMB substrate were used directly from Ready-Set-Go Mouse Ig kits (eBioscience,

NIH-PA Author Manuscript

NIH-PA Author Manuscript

NIH-PA Author Manuscript

San Diego, CA). For detection of **5a-**, **5-**, or **1**-specific antibodies by ELISA, 50 μL of 0.01 mg/mL **5a** or **5**, and 50 μL of 0.1 mg/mL **2** were incubated overnight at 4°C. Capture antibodies were incubated according to manufacturer's instructions. For washing, 1% PBST (1% BSA (w/v) and 0.05% (v/v) Tween 20 in PBS) was used. Blocking (4 h, RT) and serum dilutions (100 μL total incubation volume) were performed with 2% PBST (2% BSA (w/v) and 0.05% (v/v) Tween 20 in PBS). After washing five times, HRP-conjugated antibody was incubated at RT for 3 h, and detection performed as per manufacturer's instruction. Serum from all experimental mice plus serum from an untreated but WSN-infected mouse (positive control collected at 2.5 weeks p.i.) were included on each plate. Sensitivity of the assay was 1.5 ng/mL for IgG, 0.7 ng/mL for IgM, and 0.7 ng/mL for IgA.

Ferret experiments

Adult male Fitch ferrets, five months of age (Triple F Farms, Sayre, PA), serologically negative by hemagglutination-inhibition assay for currently circulating influenza viruses, were used in this study. Six ferrets per group were anesthetized with an intramuscular injection of a ketamine hydrochloride (24 mg/kg)-xylazine (2 mg/kg)-atropine (0.05 mg/kg) cocktail and infected intranasally with Nanchang virus at 10^5 EID_{50} in a final volume of 1 mL of PBS. Ferrets were sedated by ketamine before intranasal delivery of 500 μL (250 μL per nostril) of 6 μmol/kg bodyweight of high-molecular-weight **5a** in PBS; six control ferrets received vehicle (PBS) only. Ferrets receiving treatment with **1** were given 0.7 μmol/kg bodyweight - equimolar to the dose of **5a** on a **1**-basis - in PBS administered intranasally. The animals received daily dosing of PBS, **5a**, or **1** over a period of eight days beginning 24 h p.i. Ferrets were monitored daily for changes in body weight and temperature, as well as clinical signs of illness. Body temperatures were measured using an implantable subcutaneous temperature transponder (BioMedic Data Systems, Seaford, DE). Virus shedding was measured in nasal washes collected p.i. on days 2, 4, 6, and 8 from anesthetized ferrets as previously described (20). Virus titers in nasal washes were determined in eggs and expressed as EID_{50}/mL.

Statistical analysis

Unpaired two-tailed Student's *t*-test was performed using Prism 6 software.

RESULTS AND DISCUSSION

Poly-*L*-glutamine-attached zanamivir **5a** (Figure 1A) is a far more potent inhibitor of influenza A virus than **1** itself due to the multivalency effect (9,12). Its structure comprises the neuraminidase inhibitor **1**, the biodegradable linear polypeptide, and a linker group between them (Figure 1). In the first phase of this work, we have pursued *in vitro* SAR studies of the linker group and the polymer backbone in 10 mole-percent polymeric conjugates.

Masuda *et al.*'s SAR study of derivatives of **1** found that modification of the 7-OH group with alkyl ether substituents less than ten carbon atoms in length (nominally some 16 Å) had no negative effects on antiviral activity compared to **1** itself (9). Subsequent conjugation of such derivatives to a poly-*L*-glutamine scaffold greatly enhanced antiviral activity (9). Therefore, we first selected a linker of only six carbon atoms in length (Figure 1B, compound **2**) and additionally examined two alternative linker structures of approximately the same 10 Å length: (i) a rigid hydrophobic phenyl moiety and (ii) a flexible and hydrophilic ethylene glycol moiety (Figure 1B, compounds **3** and **4**, respectively).

We tested these analogs of **1** in the plaque reduction assay against three distinct strains of influenza virus: influenza A/WSN/33 (WSN), human influenza A/Wuhan/359/95 (Wuhan),

NIH-PA Author Manuscript

NIH-PA Author Manuscript

NIH-PA Author Manuscript

and avian influenza A/turkey/MN/833/80 (TKY). For all three strains, IC_{50} (half of maximal inhibitory concentration) values showed that **2** was the most potent inhibitor by up to 6-fold over flexible hydrophilic analog **3** and 50-fold over rigid analog **4** (Table I). When attached to the poly-*L*-glutamine backbone, compound **5a** – the polymeric conjugate of **2** (Figure 1D) – was at least as good as either **5b** or **5c** against Wuhan, but not necessarily WSN virus, and approximately 10-fold more potent against TKY virus (Table I). Thus, we selected analog **2**, which is flexible and moderately hydrophobic, for subsequent SAR studies of the polymeric conjugates.

Next, we examined the effect of the length and charge of the polymeric backbone on antiviral activity. Specifically, poly-*L*-glutamate of either 3–15 kDa (~20–100 repeating units) or 50–100 kDa (~330–660 repeating units) was used as a scaffold to which 10 mole-percent of **2** was then conjugated. Subsequently, the glutamate side chains were modified with ammonia or choline groups to impart a neutral or zwitter-ionic charge state, respectively (Fig. 1E). We assessed the inhibitory potency of these six polymeric conjugates in the plaque assay with Wuhan, wild-type TKY, and **1**-resistant (E119D) TKY influenza strains. Conjugate **7a**, regardless of molecular weight or viral strain, had the highest IC_{50} value (Figure 2). For negatively charged conjugate **6a**, the low-molecular-weight inhibitor had an IC_{50} of up to 4-fold lower than the high-molecular-weight conjugate against all three viruses. Conversely, high-molecular-weight **5a** was up to 15-fold more potent than the low-molecular-weight variant and up to 75-fold more potent compared to the corresponding charged analogs **6a** and **7a**.

In their study of sialic-acid-derivatized polyacrylamides that bind the hemagglutinin of influenza virus, the Whitesides group reported that addition of a charge – whether positive or negative – to the backbone decreased binding in an erythrocyte sedimentation assay (21,22). Our results herein suggest that the same trend applies to neuraminidase-binding poly-*L*-glutamate-based conjugates of **2** in the plaque reduction assay. Overall, conjugate **5a** with its long neutral backbone and short flexible linker is the most potent inhibitor of the derivatives examined herein *in vitro*.

In the second (*in vivo*) phase of this study, we tested high-molecular-weight **5a** in a mouse model of influenza virus infection using two strains of influenza virus: WSN and A/PR/8/34 (PR8). Mice were given doses of polymeric **5a**, small-molecule **1**, or PBS (as a control) intranasally, immediately followed by intranasal infection. At 6, 24, and 48 h post-infection (p.i.), the mice were again given **5a, 1**, or PBS intranasally (Figure 3A). Viral load was measured in lung homogenates at 72 h p.i.

We determined viral titers from lung homogenates of WSN-infected mice using the plaque assay. Untreated mice had high titers of 10^7 pfu/mL (Figure 3B). When treated with **1**, the titers dropped 20-fold. Upon treatment with a molar equivalency (in terms of **1**) of polymeric conjugate **5a**, the titers plummeted 190-fold, whereas no decrease was detected from treatment with poly-*L*-glutamine (**5**) alone. Thus **5a** is some 10-fold more potent than **1** at inhibiting WSN infection in mice.

For mice infected with PR8, we analyzed lung homogenates using qRT-PCR. Here, treatment with **5a** reduced viral load 11-fold more than that with **1** (Figure 3C), which correlated well with the above-referenced WSN study. Across all influenza strains and analytical methods, therefore, we observed the same trend: polymeric conjugate **5a** was an order of magnitude more potent than small-molecule **1**.

In mice, intranasal p.i. delivery of fluids with influenza virus – as in this study – had been shown to exacerbate the disease (23). This fact could render experimental compounds less

NIH-PA Author Manuscript

NIH-PA Author Manuscript

NIH-PA Author Manuscript

potent because they must inhibit significantly higher viral titers than presumed (23). Consequently, our data may even underestimate the potency of polymeric inhibitor **5a** in the mouse model.

Next, we determined the efficacy of high-molecular-weight **5a** in ferrets because this animal model of influenza infection accurately reflects virus infectivity and antiviral activities in humans (24,25). On day 0, ferrets were infected with A/Nanchang/933/95 (Nanchang) virus, a clinically relevant human influenza strain. Beginning one day p.i., the ferrets were dosed daily with **5a, 1**, or PBS (as a control). A nasal wash was collected from each ferret on days 2, 4, 6, and 8 to measure viral titer. On day 2 p.i., the ferrets given equimolar doses of **1** or **5a** (in terms of **1**) exhibited similar reductions in titer of 38- and 30-fold, respectively, compared to the PBS-treated group. Treatment with **5a** continued to reduce viral titers significantly compared to PBS controls – 30- and 20-fold on days 4 and 6 p.i., respectively, – whereas treatment with **1** did not. Thus, polymeric conjugate **5a** is a more effective therapeutic agent than **1** in this highly relevant ferret model of influenza infection.

Finally, we examined whether repeated dosing with high-molecular-weight **5a** induced immune responses, which could render **5a** ineffective. Although small molecules, such as **2**, do not typically elicit an antibody response, as part of a polymeric conjugate they can behave as haptens and become immunogenic (26–28). To assess this possibility, we challenged mice intranasally for four days with a daily dose of PBS (as a control) or 40 μg of **5a** (which was 40 fold higher than what was used to inhibit virus infection in mice). Ten days after the first administration serum samples were collected. To increase the probability of antibody induction, after four weeks the mice were re-challenged for three days with PBS or 40 μg of **5a** daily, and sera were again collected ten days later. Using **2, 5**, and **5a** as capture antigens in an ELISA assay, we tested for the presence of specific IgG, IgM, and IgA in the serum samples. Only a background level of immunoglobulin was detected in the mice given **5a** before, after primary, and after secondary challenge, the same as in control mice given PBS (Table II). Even when **5d** with 20 mol-percent **2** was used as a capture antigen, only background levels of immunoglobulin were detected in **5a**-treated mice, as in PBS-treated mice. Thus, upon repeated challenge with a dose 40-fold higher than that used in the aforementioned infection studies, no neutralizing antibodies against **5a** or any of its components were observed.

CONCLUSION

In summary, in this study we have demonstrated that optimized polymeric drug species **5a** is an efficacious inhibitor of influenza infections in the respiratory tracts, reducing viral titers up to 190-fold *in vivo* and without stimulating an immune response. These results coupled with other beneficial properties of **5a**, namely, multiple modes of inhibition (13) and efficacy against drug-resistant virus strains (12), make it a promising inhibitor of influenza infection for further development.

Acknowledgments

We thank Amanda Souza, Ryan Phennicie, and Peter Bak for help with mouse experiments. This work was financially supported in part by National Institutes of Health grant U01-AI074443. The findings and conclusions herein are those of the authors and do not necessarily reflect the views of the funding agency.

Abbreviations

SAR	structure-activity relationship

NIH-PA Author Manuscript

NIH-PA Author Manuscript

NIH-PA Author Manuscript

WSN	influenza strain A/WSN/33
Wuhan	influenza strain A/Wuhan/359/95
TKY	influenza strain A/turkey/MN/833/80
TKY E119D	influenza strain A/turkey/MN/833/80/E119D
PR8	influenza strain A/PR/8/34
Nanchang	influenza strain A/Nanchang/933/95
p.i.	post-infection

REFERENCES

1. Dushoff J, Plotkin JB, Viboud C, Earn DJD, Simonsen L. Mortality due to influenza in the United States—an annualized regression approach using multiple-cause mortality data. Am J Epidemiol. 2005; 163:181–187. [PubMed: 16319291]
2. Graham-Rowe D. Racing against the flu. Nature. 2011; 480:S2–S3. [PubMed: 22158296]
3. Palmer R. Lines of defense. Nature. 2011; 480:S9–S10. [PubMed: 22158299]
4. Gubareva LV. Molecular mechanism of influenza virus resistance to neuraminidase inhibitors. Virus Res. 2004; 103:199–203. [PubMed: 15163510]
5. Ortigoza MB, Dibben O, Maamary J, Martinez-Gil L, Leyva-Grado VH, Abreu P, Ayllon J, Palese P, Shaw ML. A novel small molecule inhibitor of influenza A viruses that targets polymerase function and indirectly induces interferon. PLoS Pathog. 2012; 8(4):e1002668. [PubMed: 22577360]
6. Koyama K, Takahashi M, Oitate M, Nakai N, Takakusa H, Miura S, Okazaki O. CS-8958, a prodrug of the novel neuraminidase inhibitor R-125489, demonstrates a favorable long-retention profile in the mouse respiratory tract. Antimicrob Agents Chemother. 2009; 53:4845–4851. [PubMed: 19687241]
7. An J, Lee DCW, Law AHY, Yang CLH, Poon LLM, Lau ASY, Jones SJM. A novel small-molecule inhibitor of the avian influenza H5N1 virus determined through computational screening against the neuraminidase. J Med Chem. 2009; 52:2667–2672. [PubMed: 19419201]
8. Jablonski JJ, Basu D, Engel DA, Geysen HM. Design, synthesis, and evaluation of novel small molecule inhibitors of the influenza virus protein NS1. Bioorg Med Chem. 2012; 20:487–497. [PubMed: 22099257]
9. Masuda T, Yoshida S, Arai M, Kaneko S, Yamashita M, Honda T. Synthesis and anti-influenza evaluation of polyvalent sialidase inhibitors bearing 4-guanidino-Neu5ac2en derivatives. Chem Pharm Bull. 2003; 51:1386–1398. [PubMed: 14646315]
10. Honda T, Yoshida S, Arai M, Masuda T, Yamashita M. Synthesis and anti-influenza evaluation of polyvalent sialidase inhibitors bearing 4-guanidino-Neu5Ac2en derivatives. Bioorg Med Chem Lett. 2002; 12:1929–1932. [PubMed: 12113811]
11. Honda T, Kubo S, Masuda T, Arai M, Kobayashi Y, Yamashita M. Synthesis and *in vivo* influenza virus-inhibitory effect of ester prodrug of 4-guanidino-7-*O*-methyl-Neu5Ac2en. Bioorg Med Chem Lett. 2009; 19:2938–2940. [PubMed: 19414262]
12. Weight AK, Haldar J, de Cienfuegos LA, Gubareva LV, Tumpey TM, Chen J, Klibanov AM. Attaching zanamivir to a polymer markedly enhances its activity against drug-resistant strains of influenza A virus. J Pharm Sci. 2011; 100:831–835. [PubMed: 20740680]
13. Lee CM, Weight AK, Haldar J, Wang L, Klibanov AM, Chen J. Polymer-attached zanamivir inhibits synergistically both early and late steps of influenza virus infection. Proc Natl Acad Sci USA. 2012; 109:20385–20390. [PubMed: 23185023]
14. Haldar J, de Cienfuegos LA, Tumpey TM, Gubareva LV, Chen J, Klibanov AM. Bifunctional polymeric inhibitors of human influenza A viruses. Pharm Res. 2010; 27:259–263. [PubMed: 20013036]

NIH-PA Author Manuscript

NIH-PA Author Manuscript

NIH-PA Author Manuscript

15. Andrews DM, Cherry PC, Humber DC, Jones PS, Keeling SP, Martin PF, Shaw CD, Swanson S. Synthesis and influenza virus sialidase inhibitory activity of analogues of 4-guanidino-NeuAc2en (Zanamivir) modified in the glycerol side-chain. Eur J Med Chem. 1999; 34:563–574. [PubMed: 11278042]

16. Reed LJ, Muench H. A simple method of estimating fifty percent endpoints. Am J Hygiene. 1938; 27:493–497.

17. van Elden LJR, Nijhuis M, Schipper P, Schuurman R, van Loon AM. Simultaneous detection of influenza viruses A and B using real-time quantitative PCR. J Clin Microbiol. 2001; 39:196–200. [PubMed: 11136770]

18. Smith JS, Tian J, Lozier JN, Byrnes AP. Severe pulmonary pathology after intravenous administration of adenovirus vectors in cirrhotic rats. Molec Ther. 2004; 9:932–941. [PubMed: 15194060]

19. Zhang L, Hartshorn KL, Crouch EC, Ikegami M, Whitsett JA. Complementation of pulmonary abnormalities in SP-D(−/−) mice with an SP-D/conglutinin fusion protein. J Biol Chem. 2002; 277:22453–22459. [PubMed: 11956209]

20. Zitzow LA, Rowe T, Morken T, Shieh WJ, Zaki S, Katz JM. Pathogenesis of avian influenza A (H5N1) viruses in ferrets. J Virol. 2002; 76:4420–4429. [PubMed: 11932409]

21. Mammen M, Dahmann G, Whitesides GM. Effective inhibitors of hemagglutination by influenza virus synthesized from polymers having active ester groups. Insight into mechanism of inhibition. J Med Chem. 1995; 38:4179–4190. [PubMed: 7473545]

22. Sigal GB, Mammen M, Dahmann G, Whitesides GM. Polyacrylamides bearing pendant α-sialoside groups strongly inhibit agglutination of erythrocytes by influenza virus: the strong inhibition reflects enhanced binding through cooperative polyvalent interactions. J Am Chem Soc. 1996; 118:3789–3800.

23. Smee DF, von Itzstein M, Bhatt B, Tarbet EB. Exacerbation of influenza virus infections in mice by intranasal treatments and implications for evaluation of antiviral drugs. Antimicrob Agents Chemother. 2012; 56:6328–6333. [PubMed: 23027194]

24. Bouvier NM, Lowen AC. Animal models for influenza virus pathogenesis and transmission. Viruses. 2010; 2:1530–1563. [PubMed: 21442033]

25. Belser JA, Katz JM, Tumpey TM. The ferret as a model organism to study influenza A virus infection. Disease Models Mechanisms. 2011; 4:575–579. [PubMed: 21810904]

26. Lemus, R.; Karol, MH. Conjugation of haptens. In: Jones, ME.; Lympany, P., editors. Methods in Molecular Medicine, Vol. 138: Allergy Methods and Protocols. Totowa, NJ: Humana Press; 2008. p. 167-182.

27. Sylvia, LM. Drug allergy, pseudoallergy, and cutaneous diseases. In: Tisdale, JE.; Miller, DA., editors. Drug-Induced Diseases, Prevention, Detection, and Management. Bethesda, MD: American Society of Health-System Pharmacists; 2010. p. 57-61.

28. Mansour, NA.; Alassuity, AS. Immunoassays for the detection of pesticides. In: Valdes, JJ.; Sekowski, JW., editors. Toxicogenomics and Proteomics, Vol. 356: NATO Science Series, I: Life and Behavioural Sciences. Lansdale PA: IOS Press; 2004. p. 159-180.

NIH-PA Author Manuscript

NIH-PA Author Manuscript

NIH-PA Author Manuscript

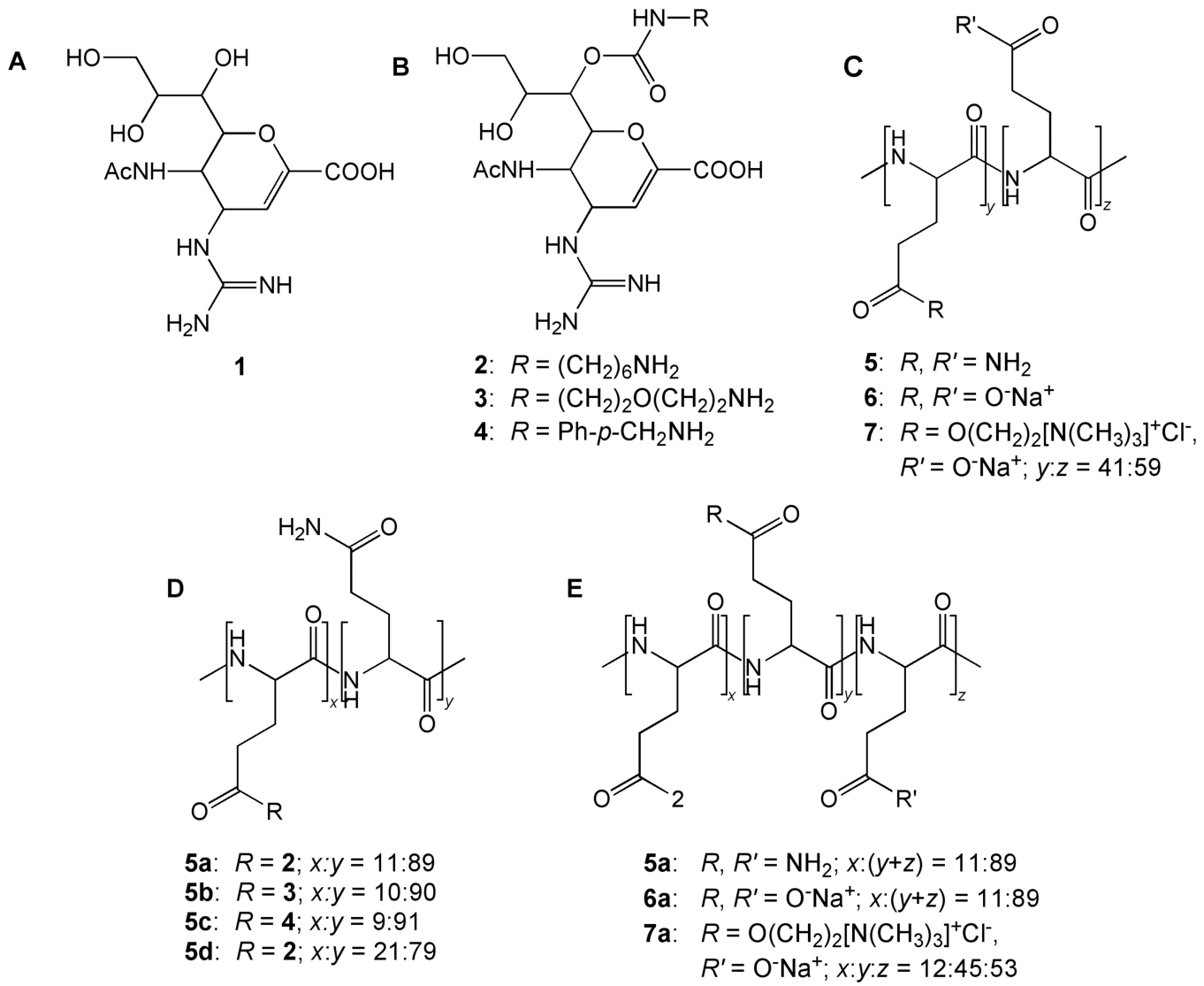

Figure 1.

Chemical structures (**A**) of zanamivir itself (**1**) and (**B**) of its derivatives with different linkers (**2–4**) for attachment to (**C**) polymer scaffolds with different electrostatic charges (neutral, negative, and zwitter-ionic) (**5–7**) to give polymer conjugates with (**D**) varying linker groups (**5a–5c**) and (**E**) charges on the polymer backbone (**5a–7a**).

NIH-PA Author Manuscript
NIH-PA Author Manuscript
NIH-PA Author Manuscript

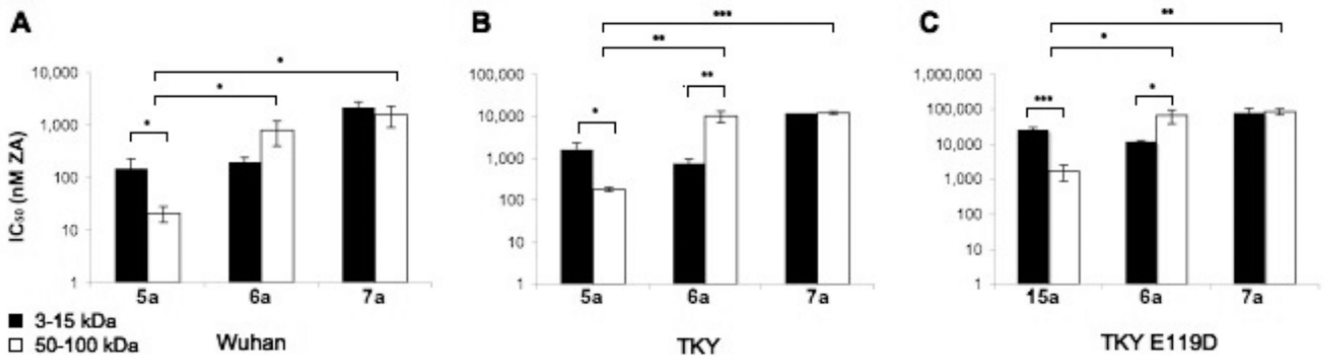

Figure 2.

IC_{50} values for low-molecular-weight (3–15 kDa; black bars) and high-molecular-weight (50–100 kDa; white bars) conjugates **5a–7a** against (**A**) Wuhan, (**B**) TKY, and (**C**) TKY E119D isolates of influenza A virus. IC_{50} values, reported as nanomolar concentrations of **1**, were determined using the plaque reduction assay after pre-incubation of virus and polymer. Thus, IC_{50} values reflect inhibition of infection. Since IC_{50} values of bare backbones **5–7** ranged from 2 to 39 mM, compared to at least 85 μM for drug conjugates, the polymers themselves had no appreciable antiviral activity. The IC_{50} values for high-molecular-weight **5a** (50–100 kDa) against Wuhan, TKY, and TKY E119D isolates, previously reported by us (11), are included herein for comparison purposes. * $p < 0.05$, ** $p < 0.01$, and *** $p < 0.001$ were determined by a two-tailed Student's *t*-test. All reported values are the mean ± SD of at least three independent measurements.

NIH-PA Author Manuscript

NIH-PA Author Manuscript

NIH-PA Author Manuscript

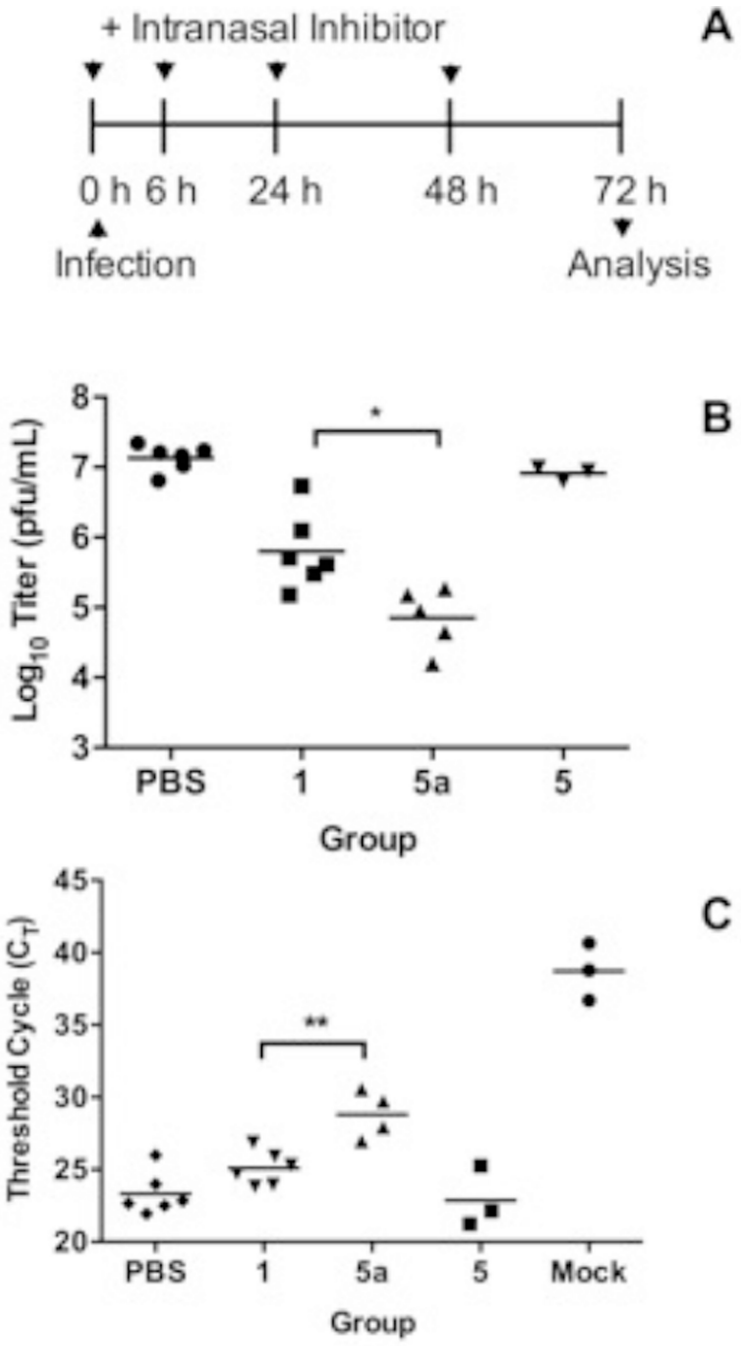

Figure 3.

(**A**) Experimental design to determine the efficacy of **5** and **5a** in mice. (**B**) Viral titers (pfu/mL) from plaque assay of lung homogenates from mice infected with the WSN strain. Equimolar doses of **1** and **5a** were used; a 40-fold higher dose of backbone **5** was included as a control. The PBS group was infected and given vehicle only. Mice were dosed intranasally, immediately infected intranasally, and dosed again at 6, 24, and 48 h p.i.; their lungs were harvested 72 h p.i. Mock-infected group, not shown here due to scale, exhibited no plaques. (**C**) Viral load in lung homogenates of mice infected with PR8 strain. C_T values (higher numbers reflect lower relative levels of viral RNA expression) from qRT-PCR of

lung homogenates. The mock group was given only the vehicle. Experimental design was the same as in part (**B**). * $p < 0.05$ and ** $p < 0.01$ were determined by two-tailed Student's *t*-test. All reported values are the mean of at least three independent measurements.

NIH-PA Author Manuscript
NIH-PA Author Manuscript
NIH-PA Author Manuscript

NIH-PA Author Manuscript

NIH-PA Author Manuscript

NIH-PA Author Manuscript

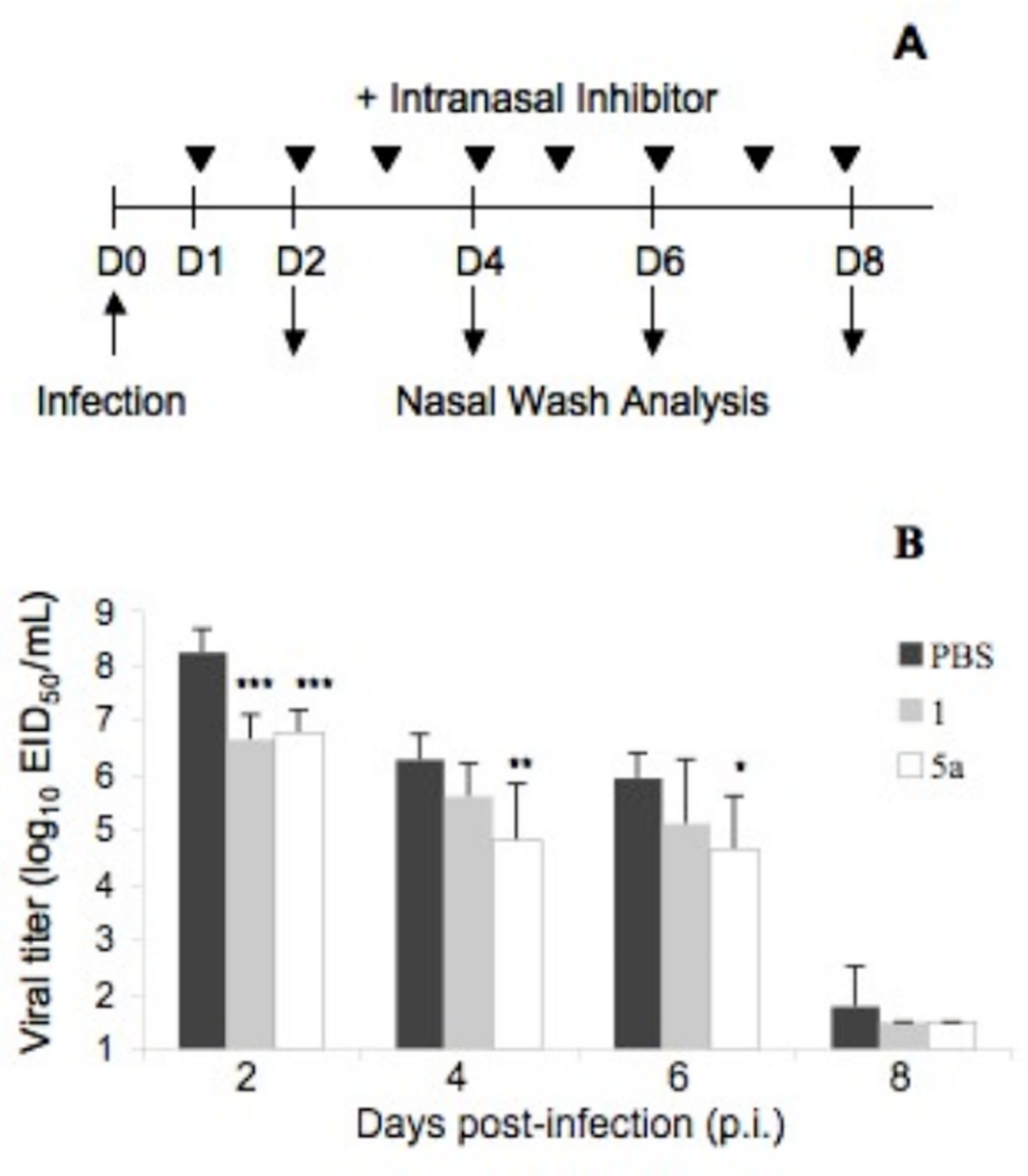

Figure 4.

(**A**) Experimental design to determine therapeutic efficacy of **5a** in ferrets. (**B**) Viral titers in nasal washings of ferrets infected with Nanchang strain of influenza virus. Groups were treated with vehicle (PBS; black bars; n=6), or equimolar doses of **1** (grey bars, n=6) or **5a** (white bars, n=6). Statistically significant differences between PBS control and treated groups are represented by * $p < 0.05$ and ** $p < 0.01$ as determined by two-tailed Student's *t*-test. Mean values ± SEM represent triplicate measurements.

NIH-PA Author Manuscript
NIH-PA Author Manuscript
NIH-PA Author Manuscript

Table I

Antiviral activities of **1**'s analogs **2–4** and their polymer-attached derivatives **5a–5c** against three strains of influenza A virus, as determined by the plaque reduction assay.

Inhibitor	IC_{50} (nM 1)[a]		
	WSN	Wuhan[b]	TKY[b]
2	$(1.0 \pm 0.4) \times 10^4$	$(4.3 \pm 0.20) \times 10^5$	$(4.3 \pm 1.1) \times 10^4$
3	$(5.7 \pm 3.9) \times 10^4$	$(1.3 \pm 0.56) \times 10^6$	$(1.4 \pm 0.34) \times 10^6$
4	$(7.6 \pm 1.3) \times 10^4$	$(8.4 \pm 1.3) \times 10^5$	$(2.3 \pm 0.71) \times 10^6$
5a	$(1.8 \pm 0.5) \times 10^2$	21 ± 7.3	$(1.8 \pm 0.20) \times 10^2$
5b	$(1.3 \pm 0.80) \times 10^2$	$(1.5 \pm 0.63) \times 10^2$	$(1.5 \pm 0.70) \times 10^3$
5c	81 ± 1.0	43 ± 23	$(9.8 \pm 1.2) \times 10^3$

[a] Reported values were determined from experiments run at least in triplicate. The IC_{50} values (± SD) are expressed as nanomolar concentrations of **1**, whether free or conjugated to poly-*L*-glutamine. To determine the IC_{50} values, inhibitor and influenza viruses were incubated together prior to the plaque assay. Therefore, the IC_{50} values reflect inhibition of infection. The IC_{50} values for unmodified poly-*L*-glutamine ranged from 2 to 14 mM (on a monomer basis), indicating that the polymer itself had no appreciable antiviral activity.

[b] The IC_{50} values for compounds **2** and **5a** against Wuhan and TKY strains, previously reported by us (12), are included here for comparison.

NIH-PA Author Manuscript NIH-PA Author Manuscript NIH-PA Author Manuscript

Table II

Drug-specific serum immunoglobulin ELISA titers from mice treated with high-dose **5a** or PBS (as a control) were measured pre-challenge (“Pre-“), 10 days after primary challenge (“Primary”), and 10 days after secondary challenge (“Secondary”).

Capture antigen	Time point (relative to challenges)	Reciprocal specific antibody titers[a]					
		IgG		IgM		IgA	
		PBS	5a	PBS	5a	PBS	5a
1	Pre-	<20	<20	<20	<20	<20	<20
	Primary	<20	<20	<20	<20	<20	<20
	Secondary	<20	<20	20	20	<20	<20
5	Pre-	<20	<20	20	20	20	20
	Primary	<20	<20	20	20	20	20
	Secondary	<20	<20	20	20	20	20
5a	Pre-	<20	<20	<20	<20	<20	<20
	Primary	<20	<20	20	<20	20	<20
	Secondary	<20	<20	20	20	20	20
5b	Pre-	<20	<20	40	40	20	20
	Primary	<20	<20	40	20	20	20
	Secondary	<20	<20	40	40	20	20

[a]The titers are reported as the reciprocal of the least dilute sample with signal 2-fold above background and are the average of at least two measurements of each sample within each group (n=3). Serum dilutions were 1:20, 1:40, and 1:100.